Structure and Properties of (1−*x*)PZN−*x*PT Thin Films with Perovskite Phase Promoted by Polyethylene Glycol

Shuhui Yu,[†,‡] Kui Yao,*[,†] and Francis Eng Hock Tay[‡]

Institute of Materials Research and Engineering (IMRE), 3 Research Link, Singapore 117602, and Faculty of Engineering, National University of Singapore, 10 Kent Ridge Crescent, Singapore 119260

Received November 17, 2005. Revised Manuscript Received August 27, 2006

Perovskite ferroelectric (1−*x*)$Pb(Zn_{1/3}Nb_{2/3})O_3$−*x*$PbTiO_3$ ((1−*x*)PZN−*x*PT) thin films were prepared on $LaAlO_3$ (LAO) substrates with a polyethylene glycol (PEG)-modified sol−gel method. It was found that the introduction of the PEG in the precursor solutions dramatically promoted the formation of the perovskite phase while suppressing the pyrochlore phase. With the aid of PEG, (001)-oriented epitaxial perovskite (1−*x*)PZN−*x*PT thin films with *x* as low as 0.3 were successfully achieved without detectable pyrochlore phase. The perovskite phase was still dominant when *x* was reduced to 0.1 in which the composition is around the morphotropic phase boundary (MPB). The electric properties of our 0.7PZN−0.3PT films deposited on conductive $LaNiO_3$-coated LAO substrates were characterized, and the films exhibited good dielectric, ferroelectric, and piezoelectric properties. An understanding on the mechanism of PEG promoting the perovskite phase and suppressing the pyrochlore phase has been developed through systematic investigation in this paper.

1. Introduction

Perovskite $Pb(Zn_{1/3}Nb_{2/3})O_3$ (PZN) is a technically important relaxor ferroelectric material. When modified with $PbTiO_3$ (PT), a complete solid solution (1−*x*)$Pb(Zn_{1/3}Nb_{2/3})O_3$−*x*$PbTiO_3$ ((1−*x*)PZN−*x*PT) is formed. This (1−*x*)PZN−*x*PT solid solution has a morphotropic phase boundary (MPB) when *x* is around 0.1 at which rhombohedral and tetragonal phases coexist. Among all the perovskite-type piezoelectric materials, single-crystal (1−*x*)PZN−*x*PT with a MPB composition exhibits the most superior piezoelectric performance (d_{33} > 2000 pC) along the (001) direction.[1,2] It is thus greatly desired to obtain the superior piezoelectric property in epitaxial (1−*x*)PZN−*x*PT thin film for microsystem applications. However, synthesizing single-phase perovskite (1−*x*)PZN−*x*PT thin films with low PT content has proved to be extremely difficult due to the preferential formation of paraelectric pyrochlore phase.

Various methods, including sol−gel,[3,4] charged liquid cluster beam,[5] and metal-organic chemical vapor deposition (MOCVD),[6] have been employed to prepare the (1−*x*)PZN−*x*PT thin films. However, single perovskite phase cannot be achieved with the PT amount below 60 mol %, even using a perovskite-structured seeding layer, as reported in our previous work.[4] As a result, no satisfactory electrical or electromechanical properties have been obtained in the (1−*x*)PZN−*x*PT thin films.

In efforts to improve the chemical solution synthesis approach for oxides, recently, various kinds of polymers such as polyethylene glycol (PEG) and polyvinylpyrrolidone (PVP) have been introduced into the precursor solutions to obtain uniform powders or to solve the cracking problems in the resulting films.[7,8] Various powders including perovskite materials with complex compositions have been prepared through the polymer-modified solution precursors, such as $Pb(Ni_{1/3}Nb_{2/3})$−$BaTiO_3$ (PNN−BT),[9] $La_{0.67}Ca_{0.33}MnO_3$,[10] and $Pb(Mg_{1/3}Nb_{2/3})O_3$−$PbTiO_3$ (PMN−PT).[11,12] It has been found that the perovskite phase of the powders derived from some of the polymer-modified solution processes forms at a lower temperature compared to those from the solid-state reactions.[9,11] With a large excess of PEG, Lee et al. synthesized PZN powders with 91% perovskite phase.[13] They noted that the derived perovskite phase was stabilized with PEG added in the precursor. However, the mechanism of the effects of PEG on promoting the formation of the perovskite phase has not been understood.

Since randomly oriented polycrystalline (1−*x*)PZN−*x*PT ceramic does not exhibit the extraordinary strong piezoelectric effect as in its single crystal along the ⟨001⟩ direction, preparation of (001)-oriented PZN−PT thin film is more

* To whom correspondence should be addressed. Tel.: 65-68745160. Fax: 65-68720785. E-mail: k-yao@imre.a-star.edu.sg.
† IMRE.
‡ National University of Singapore.

(1) Kuwata, J.; Uchino, K.; Nomura, S. *Ferroelectrics* **1981**, *37*, 579.
(2) Kuwata, J.; Uchino, K.; Nomura, S. *Jpn. J. Appl. Phys.* **1982**, *21*, 1298.
(3) Teowee, G.; McCarThy, K. C.; McCarThy, F. S.; Davis, D. G.; Dawley, J. T.; Zelinski, B. J. J.; Uhlmann, D. R. *Mater. Res. Soc. Symp. Proc.* **1998**, *493*, 445.
(4) Yu, S.; Yao, K.; Tay, F. E. H. *Chem. Mater.* **2004**, *16*, 346.
(5) Yang, Y.; Kim, K.; Choi, H. *Thin Solid Films* **2001**, *396*, 97.
(6) Kamisuki, Y.; Taniguchi, T.; Takenaka, T. *Microelectron Eng.* **1995**, *29*, 169.
(7) Takenaka, S.; Kozuka, H. *Appl. Phys. Lett.* **2001**, *79*, 3485.
(8) Kozuka, H.; Kajimura, M. *J. Am. Ceram. Soc.* **2000**, *83*, 1056.
(9) Uekawa, N.; Sukegawa, T.; Kakegawa, K.; Sasaki, Y. *J. Am. Ceram. Soc.* **2002**, *85*, 329.
(10) Park, H.-B.; Kweon, H.-J.; Hong, Y.-S.; Kim, S.-J.; Kim, K. *J. Mater. Sci.* **1997**, *32*, 57−65.
(11) Wan, D. M.; Wang, J.; Ng, S. C.; Gan, L. M. *J. Mater. Res.* **1999**, *14*, 537.
(12) Babooram, K.; Ye, Z.-G. *Chem. Mater.* **2004**, *16*, 5365.
(13) Lee, W. S.; Isobe, T.; Senna, M. *Adv. Powder Technol.* **2002**, *13*, 43.

10.1021/cm052536v CCC: $33.50
Published on Web 10/03/2006

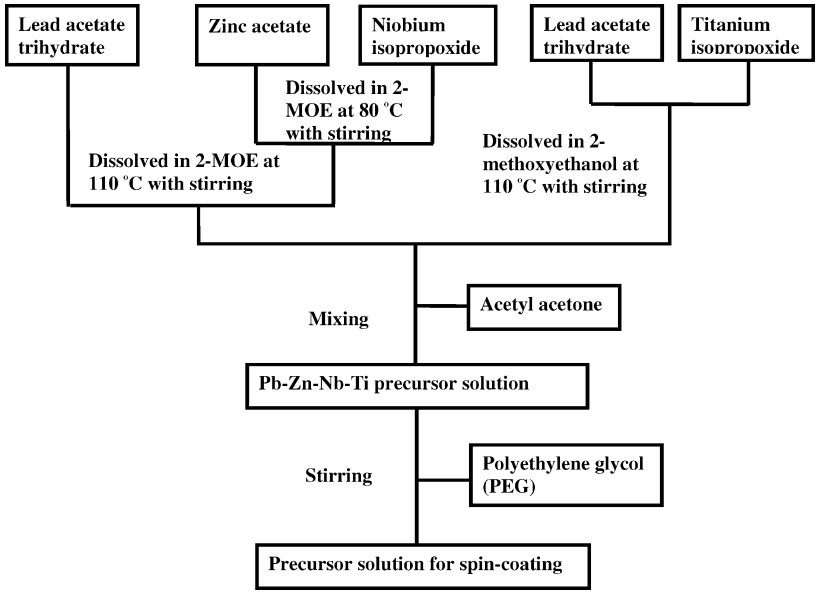

Figure 1. Flow chart for the preparation of PZN−PT precursor solution with addition of PEG.

technologically desired. In the thin film preparation, polymers are added into the solution precursor for the purpose of obtaining crack-free films with uniformly distributed grain size.[14,15] In our previous work on the study of $Pb(Zr,Ti)O_3$ (PZT) thin films,[15] we noted that the perovskite phase formed at a lower temperature when PEG was added into the solution. Acceleration of the crystallization in perovskite thin films prepared from polymer-modified precursor has also been observed by other researchers in preparing $LaMnO_3$ thin films.[16,17] These phenomena intrigue us for investigating the effects of PEG on the crystallization process of perovskite ferroelectric thin films, especially $(1-x)$PZN−xPT, in which it is extremely difficult to obtain perovskite structure but they potentially have superior performance.

Therefore, the purposes of this study are to enhance the perovskite phase in (001)-oriented epitaxial $(1-x)$PZN−xPT thin films using PEG to modify the solution precursor and develop an understanding of the mechanism of the interaction between PEG and the precursors. The ferroelectric and piezoelectric properties for the obtained 0.7PZN−0.3PT film are also studied for the first time.

2. Experimental Section

2.1. Preparation of $(1-x)$PZN−xPT Thin Films. To prepare the PZN−PT thin films, lead acetate trihydrate, zinc acetate, niobium isopropoxide, titanium isopropoxide, and 2-methoxyethanol (2-MOE) solvent were used as starting chemicals. The detailed process for the solution precursor is illustrated in Figure 1. To compensate for Pb loss during thermal treatment and to achieve films with improved properties, a Pb excess of 15% by mole with respect to the stoichiometric amount was added.[15] PZN and PT were mixed according to the targeted compositions. Finally, $(1-x)$PZN−xPT sol precursors with x values ranging from 0.1 to 0.7 were modified with PEG with a molecular weight of 200 (PEG200). The amount of PEG200 was 60% by weight, based on the total metal oxides in the solutions. After the sol was spin-coated on LAO substrates, the wet films were dried at 100 °C, pyrolyzed at 400 °C, and annealed at a higher temperature. Desired thickness was obtained by repeating the process before the final annealing. For comparison, $(1-x)$PZN−xPT films with $x = 0.2$ were also prepared from a sol in the same way but without PEG modification.

To study the crystallization process during heat treatment, one-layer 0.8PZN−0.2PT films derived from sols with and without PEG200 modification were prepared and heat-treated at different temperatures.

To investigate the effects of PEG addition amount and PEG molecular weight on the crystallization of perovskite phase, 0.8PZN−0.2PT thin films were prepared from sols with various amounts of PEG200 and PEG with different molecular weights.

2.2. Characterization of the $(1-x)$PZN−xPT Thin Films. X-ray diffraction (XRD) (Bruker GADDS, D8-ADVANCED) was carried out to determine the crystalline phases of all the films annealed at different temperatures. Phi-scan was conducted to examine the in-plane orientation of the films. The morphology and thickness of the samples were examined using field emission scanning electron microscopy (FESEM, JSM-6700F). Fourier transform infrared spectroscopy (FTIR) was applied to investigate the changes in the films after the pyrolysis. Differential thermal analysis (DTA) and thermogravimetric analysis (TGA) were performed for the gel precursors at a heating rate of 10 °C per min in air (Universal V2. 5H TA instruments). Chemical states of the elements in the films were examined using an X-ray photoelectron spectroscopy (XPS, ESCA, 220i XL VG Scientific). The spectra data were obtained using monochromatic Al Kα source (1486.6 eV). All the binding energies at various peaks were calibrated by using the binding energy of C 1s (285.0 eV).

To measure the electrical and piezoelectric properties, a conductive $LaNiO_3$ (LNO)[18] layer was fabricated with a sol−gel method on LAO substrate followed by the deposition of another 0.7PZN−0.3PT thin film. A top electrode of Au was deposited by sputtering. The dielectric constant (K) and dielectric loss ($tg\delta$) were measured using an impedance analyzer (HP4194A). Polarization-electric field

(14) Zhang, Y.; Zhu, Y.; Tan, R.; Yao, W.; Cao, L. *Thin Solid Films* **2001**, *388*, 160.
(15) Yu, S.; Yao, K.; Shannigrahi, S.; Tay, F. E. H. *J. Mater. Res.* **2003**, *18* (3), 737.
(16) Shimizu, Y.; Murata, T. *J. Am. Ceram. Soc.* **1997**, *80*, 2702.
(17) Hwang, H. J.; Towata, A.; Awano, M.; Toriyama, M. *J. Am. Ceram. Soc.* **2001**, *84*, 2323.
(18) Yu, S.; Yao, K.; Tay, F. E. H. *Ceram. Int.* **2004**, *30* (7), 1253.

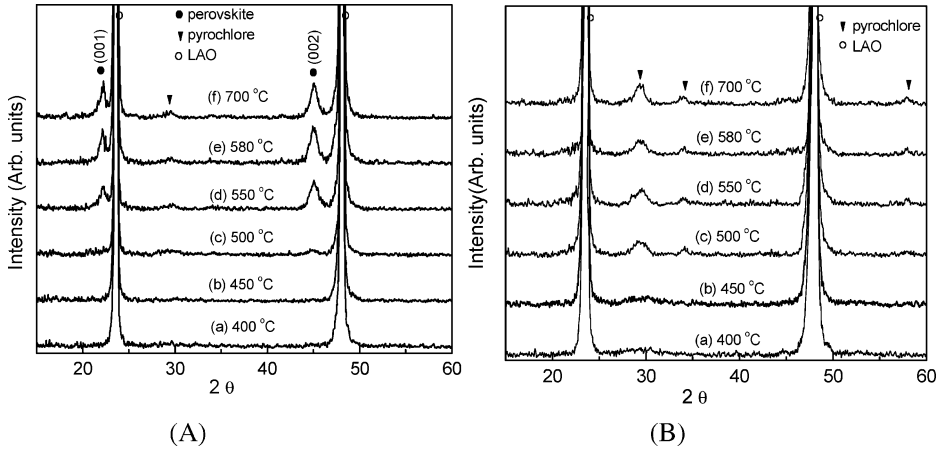

Figure 2. XRD results of the 0.8PZN−0.2PT thin films on LAO substrate derived from (A) PEG200-modified sol and (B) sol without PEG modification. Films were heated at different temperatures for 10 min.

(P-E) characteristics were measured with a RT66A testing unit connected with a high-voltage interface. The piezoelectric properties of the film were tested with a laser scanning vibrometer (LSV).[19] The film was poled at 3 V for 4 min before piezoelectric measurement.

3. Results

3.1. Crystallization of Perovskite Phase in 0.8PZN−0.2PT Thin Films Aided by PEG. Figure 2 presents the XRD results of one-layer (0.062 μm) 0.8PZN−0.2PT films prepared from the PEG200-modified sol (Figure 2A) and from the sol without PEG modification (Figure 2B). As shown in Figure 2A, for the films prepared from PEG200-modified sol, both the pyrochlore (29°) and the perovskite phases (46°) appear at 500 °C. The intensity of (001) and (002) peaks of the perovskite phase abruptly becomes high at 550 °C and the perovskite phase is dominant over the pyrochlore phase. With the increase of the heating temperature, the intensity of both the perovskite and pyrochlore phases increases. No evidence shows the transformation of pyrochlore phase into perovskite phase, even in the film annealed at 700 °C, but a slight increase of the intensity of the pyrochlore peak at 29°. The results indicate that both the perovskite and pyrochlore phases form directly from the amorphous film, and they coexist at a higher temperature.

In contrast, for the films derived from the sol without PEG modification, as shown in Figure 2B, the hump at 29° exists in the films heated at 400−450 °C, which leads to the formation of pyrochlore phase at an elevated temperature of 500 °C or above. No perovskite phase has formed even when the film was annealed at 700 °C.

The results indicate that by modification of the sol precursor with PEG, the formation of pyrochlore phase in the 0.8PZN−0.2PT films is dramatically suppressed. Dominant perovskite phase will form when the heating temperature is high enough (500 °C or above) in the film derived from the PEG-modified sol, although there is minor pyrochlore phase.

3.2. Effect of PEG Molecular Weight and Amount. Figure 3 presents the XRD patterns of the four-layer (0.25 μm) 0.8PZN−0.2PT thin films prepared from sols modified with ethylene glycol and PEG of different molecular weights. As shown in the figure, except for the film derived from the ethylene glycol-modified sol (Figure 3a), perovskite phase forms in all the films derived from the sols modified with PEG of different molecular weights (Figures 3b−3e), although minor pyrochlore phase coexists. The intensity of the XRD peaks for perovskite phase is the strongest for the film prepared from the sol modified with PEG200. The results indicate that only PEG but not its monomer ethylene glycol can promote the formation of the perovskite phase while suppressing the pyrochlore phase. Among all the polymeric species employed, PEG200 is the most efficient in suppressing the pyrochlore phase.

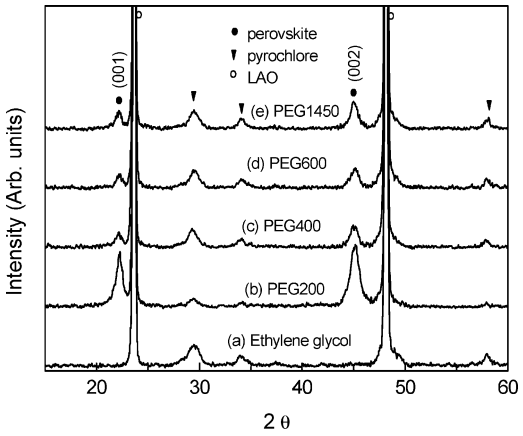

Figure 3. XRD patterns of the 0.8PZN−0.2PT thin films on LAO substrates, prepared from sols modified with 30 wt % of ethylene glycol and PEG of different molecular weights; films were annealed at 580 °C for 10 min.

Figure 4 shows the XRD patterns of the four-layer (~0.25 μm) 0.8PZN−0.2PT thin film prepared from the sols with different amounts of PEG200. As shown in this figure, perovskite phase tends to be stabilized with increasing PEG amount, and the intensity of perovskite peaks is the strongest while the intensity of the pyrochlore peaks the weakest when PEG200 is 60 wt %. However, when PEG amount is above 60 wt %, the intensity of pyrochlore peaks tends to increase again. The results indicate that 60 wt % of PEG200 is the optimal amount to form perovskite phase in the 0.8PZN−0.2PT thin film.

(19) Yao, K.; Tay, F. E. H. *IEEE Trans. Ultrason. Ferroelectr. Freq. Contr.* **2003**, *50*, 113.

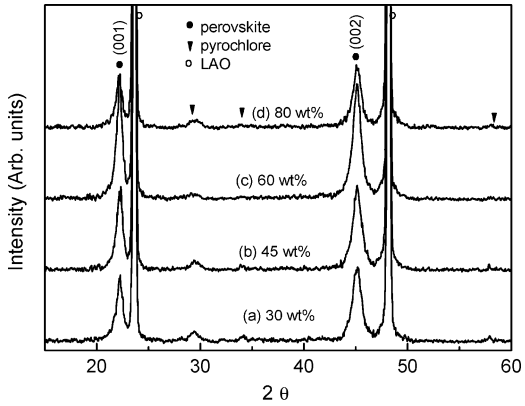

Figure 4. XRD patterns of 0.8PZN−0.2PT films prepared from sols modified with different amounts of PEG200; films were annealed at 580 °C for 10 min.

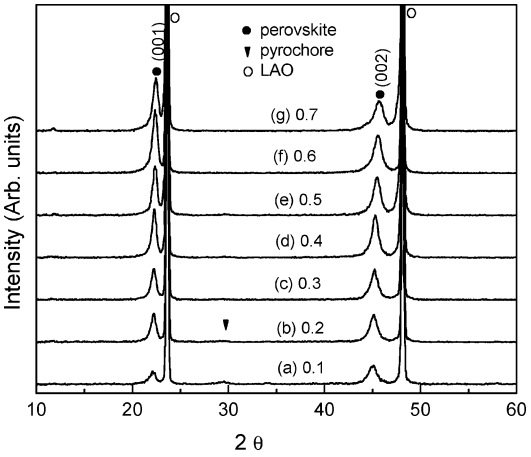

Figure 5. XRD patterns of (1−*x*)PZN−*x*PT films derived from PEG200-modified sol with *x* from 0.1 to 0.7; films were annealed at 580 °C for 10 min.

3.3. (1−*x*)PZN−*x*PT Thin Films with Different PT Content. Figure 5 presents the $\theta-2\theta$ scan of the four-layer (1−*x*)PZN−*x*PT ($x = 0.1-0.7$) films with a thickness around 0.25 μm prepared from sols modified with PEG200 on the LAO substrates. The films were annealed at 580 °C for 10 min. As shown in this figure, the perovskite phase forms in all the (1−*x*)PZN−*x*PT films with $x = 0.1-0.7$, and the perovskite phase tends to be stabilized with increased PT amount. The perovskite phase was dominant over the pyrochlore phase even in the 0.9PZN−0.1PT film. The films with $x = 0.3-0.7$ apparently show single perovskite phase.

Phi-scan shows that all the perovskite phases in our (1−*x*)PZN−*x*PT thin films are also in-plane-oriented, as one example presented in Figure 6.

3.4. Morphology of 0.8PZN−0.2PT Thin Films. Figure 7 presents the SEM images of the surfaces of the four-layer (0.25 μm) 0.8PZN−0.2PT thin films on LAO substrate prepared from the sol without PEG modification and from the sol modified with 60 wt % of PEG200. The films were annealed at 700 °C for 10 min. As shown in Figure 7A, the film derived from the sol without PEG exhibits a very rough morphology with nonuniform grain size ranging from 100 nm to even near 1 μm. In contrast, the film derived from the PEG200-modified sol has a much finer morphology and the grain size is much smaller (below 100 nm) as shown in Figure 7B. As indicated by the XRD results for the films without and with PEG addition, the large grains in Figure 7A are pyrochlore phase, while the small grains in Figure 7B are perovskite phase.

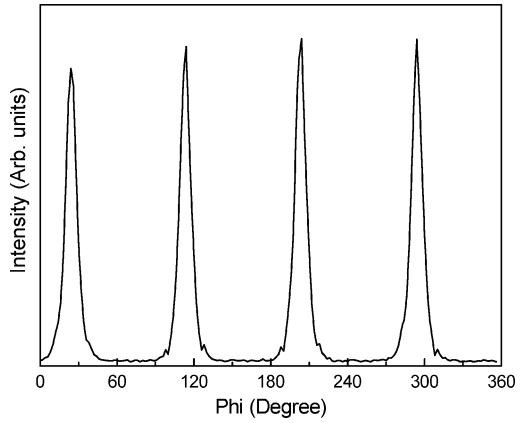

Figure 6. Phi-scan pattern of the (110)-plane of the 0.8PZN−0.2PT film prepared from the PEG200-modified sol.

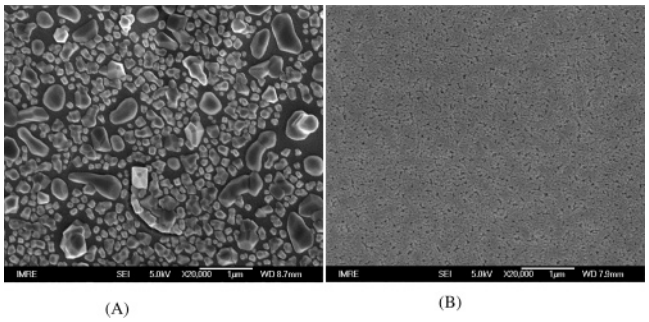

Figure 7. SEM surface morphology of four-layer (0.25 μm) 0.8PZN−0.2PT film on LAO substrates derived from different sols: (A) without PEG modification; (B) with 60 wt % PEG200 modification. Films were annealed at 700 °C for 10 min.

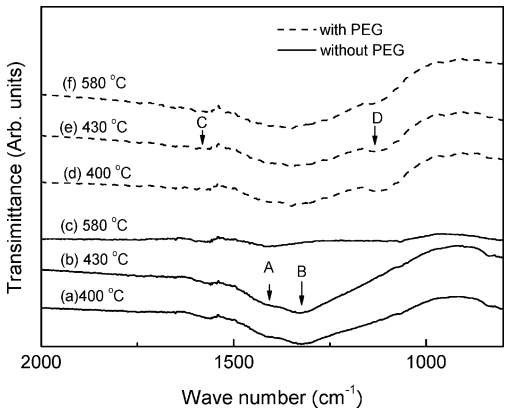

Figure 8. FTIR spectra of the 0.8PZN−0.2PT thin films on LAO substrate without and with PEG modification. (A) and (B): carbonates stretching mode; (C): H−O−H bending mode; and (D): vibration mode of the C−O−C group.

3.5. FTIR of the 0.8PZN−0.2PT Thin Films. Figure 8 shows the FTIR spectra of the 0.8PZN−0.2PT thin films derived from the sols with and without PEG modification. For the films without PEG and pyrolyzed at 400 and 430 °C, the deep valleys at 1300−1500 cm^{-1}, as shown in (a) and (b), are usually associated with C−O bond stretching in inorganic carbonates.[20] The valleys disappeared when the film was annealed at 580 °C (Figure 8c). In contrast, for the films derived from the sol modified with PEG, there are no such deep valleys between 1300 and 1500 cm^{-1} (Figures

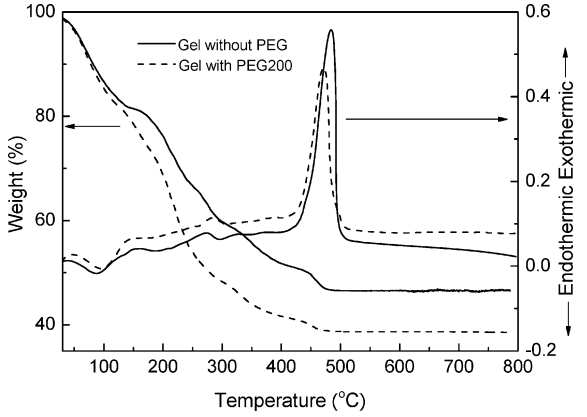

Figure 9. TGA/DTA profiles of 0.8PZN−0.2PT gel precursor with and without PEG200.

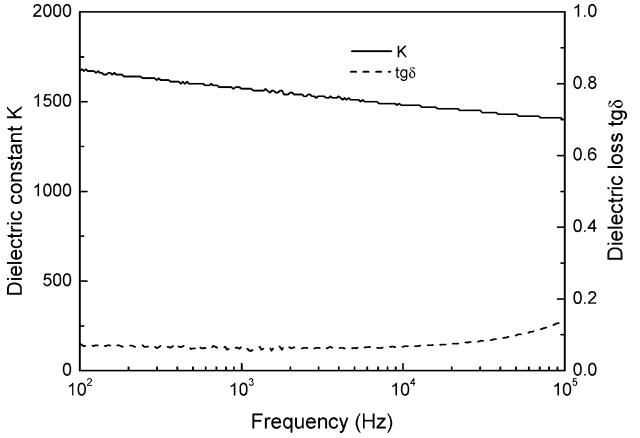

Figure 10. Dielectric constant and dielectric loss of a 0.7PZN−0.3PT film on LNO-coated LAO substrate prepared from the sol modified with PEG200; annealed at 700 °C for 10 min.

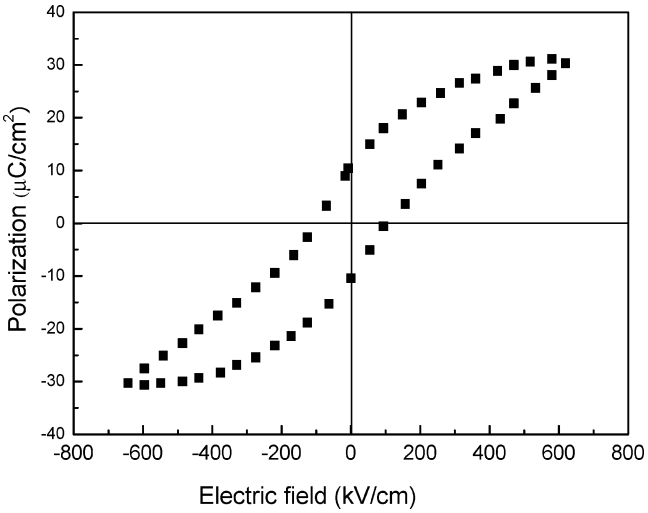

Figure 11. P-E hysteresis loop of the 0.7PZN−0.3PT film on LNO-coated LAO substrate prepared from the sol modified with 60 wt % of PEG200; annealed at 700 °C for 10 min.

8d−8f). The spectrum does not change significantly in this range when the film annealing temperature is increased from 400 to 580 °C, where the XRD results show that the films crystallized into dominant perovskite phase. A C−O−C vibration mode around 1100 cm^{-1} is only observed in the films derived from PEG-modified sol, which became weakened after the film was annealed at 580 °C. The C−O−C connections probably come from the PEG structure and they exist even at a temperature well above the decomposition temperature of pure PEG, which is below 300 °C. It is possibly due to the interaction between C−O−C and the metal ions. The FTIR results thus show that, without PEG, carbonates tend to form in the film. In contrast, C−O−C from PEG possibly interacts with metal ions, which could prevent the formation of carbonates.

3.6. TGA/DTA of the Gel Precursor. Figure 9 shows the TGA/DTA profiles for the 0.8PZN−0.2PT gel precursors with and without PEG. The difference in the final weights between the two TGA curves is due to the existence or nonexistence of PEG. For the sample with PEG, there is a sharp weight loss at 200−250 °C, corresponding to the decomposition of PEG. The subsequent weight loss with the increased temperature is continuous until the weight loss is completed at 450 °C. In contrast, for the sample without PEG, the weight loss is moderate and continuous in the range of 250−440 °C, but a sharp weight loss occurs at 440−470 °C. In reference to the FTIR results, this weight loss is attributed to the decomposition of carbonates, accompanied by the crystallization exothermic peak as shown in the DTA curve. However, there is no such stepped weight loss at 440−470 °C in the sample with PEG, implying that no or much less carbonates formed during the heating process, and the crystallization occurred at a lower temperature than the sample without PEG, as shown in the DTA curves. The results indicate that due to the interaction between metal ions and PEG, carbonate is not favored in the sample with PEG so that the crystallization occurred at a lower temperature.

3.7. Electrical Properties of 0.7PZN−0.3PT Thin Films on LAO Substrates. Since minor pyrochlore phase still exists in both 0.9PZN−0.1PT and 0.8PZN−0.2PT films while it is apparently undetectable with XRD in 0.7PZN−0.3PT film, as shown in Figure 5, a 0.7PZN−0.3PT film was prepared on LNO-coated LAO substrate for electrical testing. The thickness of the film is 0.25 μm.

Figure 10 shows the frequency dependence of dielectric constant (K) and dielectric loss ($tg\delta$) of the 0.7PZN−0.3PT film. K and $tg\delta$ are 1570 and 0.06, at 1 kHz, respectively. The dielectric constant is fairly high and the loss is quite low, which are comparable with that of the PZT films.

Figure 11 presents the P-E hysteresis loop of the film, exhibiting a remnant polarization and a coercive field of 12 $\mu C/cm^2$ and 100 kV/cm, respectively.

Figure 12 presents a three-dimensional drawing of the instantaneous vibration when the displacement of the 0.7PZN−0.3PT film reaches the maximum magnitude under a sine wave driving voltage of 4.5 V at 1.5 kHz. The central area moving upward is the Au-electrode covered area; the surrounding area moving downward below the zero point is the region without the top electrode. The dilation magnitude of the films is equivalent to the numerical addition of the displacement of the area with top electrode and the area without the top electrode.[19] Therefore, the dilation magnitude of the film, as presented in Figure 12, is around 228 pm.

(20) Lide, D. R., Ed. *CRC Handbook of Chemistry and Physics*, 72nd ed.; CRC Press: Boca Raton, FL, 1991-92; pp 97−128 (IR correlation charts).

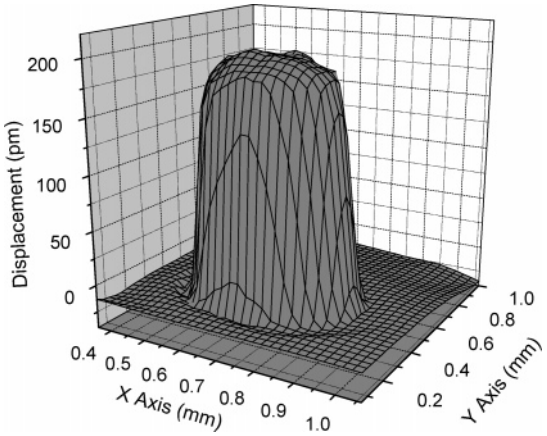

Figure 12. Three-dimensional drawing of the vibration of the 0.7PZN−0.3PT film (4.5 V, 1.5 kHz).

The effective piezoelectric coefficient d_{33} is 50.6 pm/V. Considering that the film composition of the 0.7PZN−0.3PT is not close to the MPB (∼10 mol % PT), and the quality of the epitaxial film is significantly inferior to single crystal, the relatively lower d_{33} value is understandable. Moreover, the piezoelectric dilatation magnitude of the film is reduced due to the clamping effect of the substrate. The actual piezoelectric constant should be significantly higher than this value if the real clamping effect of the substrate is taken into account.[19]

4. Discussion

To investigate the mechanism of PEG for promoting the perovskite phase while suppressing the pyrochlore phase, an understanding of the pyrochlore structure is demanded. The pyrochlore structure can be derived from fluorite structure (with a general formula BO_2), by removing $^1/_8$ of the oxygens, ordering the two cations, and ordering the oxygen vacancies.[21] As a result, there are unoccupied sites in the pyrochlore structure. It has been suggested that the lone pair $6s^2$ in the Pb^{2+} accommodate toward the vacancy.[22−24] This may explain why pyrochlore phase often forms in the synthesis of the Pb-contained ABO_3 compounds. In other words, if the directional effect of the lone pair electrons in the Pb^{2+} is weakened, the pyrochlore phase with unoccupied sites could be suppressed and hence the perovskite phase could be stabilized.

It should be noted that, unlike PEG, the ethylene glycol did not show the effects of promoting the perovskite phase as found through our experiments. There are two differences between PEG ($H(OCH_2CH_2)_n-OH$) and ethylene glycol ($HOCH_2CH_2OH$). First, PEG possesses ether oxygens (C−O−C) but ethylene glycol does not; second, PEG has a longer chain than ethylene glycol. Although many researchers insist that the interaction between PEG and metal ions is through the ether oxygens in PEG, the ether oxygen in the 2-MOE ($HOCH_2CH_2OCH_3$) solvent used in this study did not apparently exhibit any effects on the crystallization when PEG was absent. Therefore, it is the number of oxygens or the length of the PEG chains that determines how PEG interacts with metal ions and hence affects the crystallization. Among the PEGs with molecular weights ranging from 200 to 1450, PEG200 shows the most significant effect as we observed, implying that its interaction with Pb^{2+}, which could weaken the directional effect of the lone pair electrons, may be the strongest among those with different molecular weights.

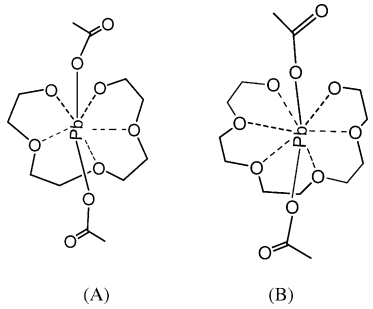

Figure 13. Local environment of Pb^{2+} in the PEG-modified precursor. (A) PEG with five oxygen donors; (B) PEG with six oxygen donors. Oxygen donors in the PEG200 arrange themselves in a nearly equatorial plane, leaving two axial sites for anion (CH_3COO^-) coordination.

As evidenced by Rogers et al.[25] with X-ray structural analysis, chelating rings often form by the connection between oxygens in the PEG and Pb ions. It is shown that not only the ether oxygens but also the oxygens in the hydroxyl are all connected to the Pb ions. There is a relationship between the chelate ring size and the metal ions radius. Izatt et al.[26,27] addressed that the crown ethers, especially the 18-membered six-donor macrocycles ($(-CH_2-O-CH_2-)_6$) are ideal for the stability of their Pb^{2+} complexes. Rogers et al.[25] also found that pentaethylene glycol (with six oxygens) is the most appropriate choice of PEG for Pb^{2+} complexation where the six oxygen donors can arrange themselves in a nearly hexagonal equatorial plane, leaving two axial sites for anion coordination. Longer chains either leave one end dangling or force unusual coordination geometries, which leave no room for anion coordination. Smaller chains result in coordinative unsaturation, which must be filled with solvent or bridging ligands. This can well explain why PEG with a molecular weight of 200 proved the most efficient in promoting the formation of the perovskite phase in our $(1-x)$PZN−xPT thin films. PEG200 has five or six donor oxygens, which can form fairly stable macrocyles with lead ions. Based on this understanding, the chelate rings formed in this study are illustrated in Figure 13.

As shown in Figure 13, by forming the equatorial rings around the Pb^{2+} ions with the anions at the two axial sites, the Pb-based complex is holodirected. Therefore, the $6s^2$ lone pair will lose its directional effects. As a result, the pyrochlore phase with oxygen vacancies is not favored. This analysis

(21) Levi, C. G. *Acta Mater.* **1998**, *46*, 787.
(22) Longo, J. M.; Raccah, P. M.; Goodenough, J. B. *Mater. Res. Bull.* **1969**, *4*, 191.
(23) Cascales, C.; Rasines, I. *Mater. Res. Bull.* **1985**, *20*, 191.
(24) Wakiya, N.; Ishizawa, N.; Shinozaki, K.; Mizutani, N. *Mater. Res. Bull.* **1993**, *28*, 137.
(25) Rogers, R. D.; Bond, A. H.; Roden, D. M. *Inorg. Chem.* **1996**, *35*, 6964.
(26) Izatt, R. M.; Bradshaw, J. S.; Nielsen, S. A.; Lamb, J. D.; Christensen, J. J. *Chem. Rev.* **1985**, *85*, 271.
(27) Izatt, R. M.; Bradshaw, J. S.; Nielsen, S. A.; Lamb, J. D.; Christensen, J. J. *Chem. Rev.* **1991**, *91*, 1721.

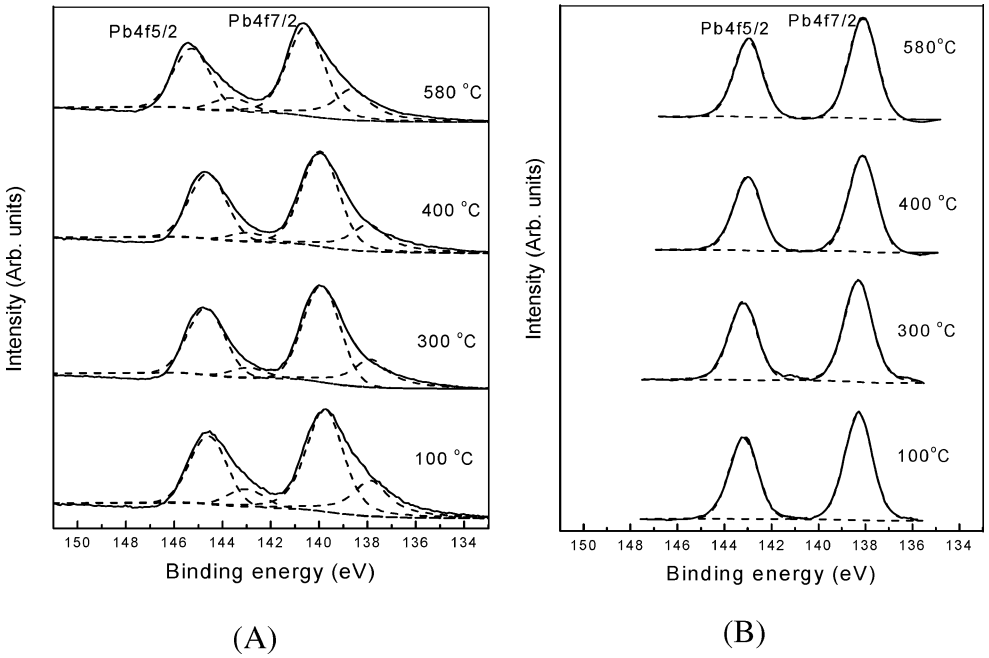

Figure 14. XPS profiles of Pb 4f in the one-layer 0.6PZN−0.4PT thin films heat-treated at different temperatures. (A) Films derived from the sol with PEG modification; (B) films derived from the sol without PEG modification. The solid lines are experimental results, and the dashed lines are fitting curves.

is consistent with the study of Shinmoni-Linvy's group[28] on the stereochemical activity of the lone pair in divalent Pb compounds. The authors found that when the coordination number of Pb is large (>6), holodirected compounds form in which the directional effects of the lone pair electrons become less evident. This trend can probably be expected on the basis of the "crowding" of the ligands.

Another effect induced by the chelate rings is that the O−Pb coordination enhances the oxidation states of the Pb^{2+} and makes the chemical state much closer to that in the perovskite phase, as confirmed by the XPS results (Figure 14). As shown in Figure 14A, there are multiple chemical states of Pb in the films with PEG modification. According to the XRD results (not shown) for the one-layer 0.6PZN−0.4PT film annealed at 580 °C, a dominant perovskite phase and a nearly undetectable pyrochlore phase coexist. Therefore, for the film annealed at 580 °C, the main peak of Pb $4f_{7/2}$ at 140.5 eV and the small peak at 138 eV represent the perovskite and pyrochlore phases in the film, respectively. Similar two peaks of Pb $4f_{5/2}$ are also observed, as shown in Figure 13A. Lee el al.'s study also shows that the binding energy of Pb 4f in perovskite phase is higher than that in pyrochlore phase.[13] It is interesting to note that the higher binding energies for the Pb 4f are also observed in the films heated at or below 400 °C, in which perovskite structure does not form yet. In contrast, for the films derived from the sol without PEG modification, there is only one peak at around 138 eV for Pb $4f_{7/2}$ in the amorphous films heated at 100 or 300 °C, and the film turns into pyrochlore phase when the film is annealed at 580 °C, as shown in Figure 10B.

For the film with PEG dried at 100 °C, the high binding energy at 139.5 eV for Pb $4f_{7/2}$ may correspond to the chemical state of Pb^{2+} interacting with PEG, while the small peak at 138 eV may represent the Pb^{2+} not interacting with PEG. Although the PEG is pyrolyzed around 300 °C, the bond between Pb^{2+} and O probably could not be broken. Therefore, the higher chemical state of Pb^{2+} remains, even when the film is heated at 300 or 400 °C, which finally leads to the formation of the perovskite phase at a higher temperature. The results imply that by forming the chelate rings around Pb^{2+} with oxygens in PEG, the electron charge in the Pb^{2+} outer shell may shift to the oxygens, which causes the binding energy of the Pb element to shift to a higher value. As a result, the ionization state of the Pb^{2+} is enhanced, thus making the chemical states of Pb^{2+} in the amorphous films closer to those in the perovskite phase. Therefore, perovskite structure is favored in the crystallization process. Results from XPS also indicate that the O−Pb chelate bonds are probably not broken during the pyrolysis process, and the oxygens coordinating to Pb^{2+} are likely brought to the perovskite structure by rearranging themselves. As supported by the FTIR results, the connections between C−O−C and Pb^{2+} may exist above 400 °C. As a result, the perovskite phase forms directly from the amorphous gel film, not through transformation from pyrochlore phase. This finding is different from the previous reports, where it is found that the perovskite phase was transformed from the pyrochlore phase in the PZN-based materials.[29,30]

A slight increase of the binding energy of Pb 4f with temperature is observed in Figure 14A, which accompanies the crystallization of the perovskite phase.

Here we just discussed the interaction between PEG and Pb^{2+}. PEG may also interact with other ions in the precursor, but the selectivity of PEG to Pb^{2+} is higher than other ions.[25,26] According to our mechanism analysis as above, the optimal molar amount of PEG added into the sol should be

(28) Shimoni-Livny, L.; Glusker, J. P.; Bock, C. W. *Inorg. Chem.* **1998**, *37*, 1853.
(29) Hu, Y. *J. Mater. Sci.* **1996**, *31*, 4255.
(30) Jang, H. M.; Oh, S. H.; Moo, J. H. *J. Am. Ceram. Soc.* **1992**, *75*, 82.

at least equal to that of Pb^{2+}. In this study, 60 wt % of PEG based on the metal oxides in the sol precursor just has the same moles as Pb^{2+}, with which the derived film exhibited the optimal crystallization of perovskite phase. The lower intensity of the XRD peaks of the films derived from the sol with 80 wt % of PEG may be caused by the pores induced by the polymers.

5. Conclusions

By modification of the sol precursor with PEG200, epitaxial $(1-x)$PZN$-x$PT thin films with (001) orientation have been successfully prepared on LAO substrates. It has been found that PEG dramatically promotes the formation of perovskite phase while suppressing pyrochlore phase. With 60 wt % of PEG200, the $(1-x)$PZN$-x$PT films with $x > 0.2$ exhibit nearly single perovskite phase. The perovskite structure is still dominant over pyrochlore phase even in 0.9PZN$-$0.1PT film. It is possible that the oxygens in the PEG interact with the Pb^{2+} through chelate rings. As a result, directional effect of the $6s^2$ lone pair in Pb^{2+} is weakened, thus suppressing the formation of pyrochlore phase. In addition, by formation of the chelation between Pb^{2+} and PEG, the chemical state of the Pb^{2+} shifts toward higher energy in the XPS spectra, which is close to the chemical state in the perovskite phase, thus facilitating its formation. As a result, the perovskite structure forms directly from the amorphous gel film but not from the transformation of a pyrochlore phase. The dramatic effects of polymer addition in the solution precursor on the crystallization process and crystal structure of an inorganic film are evident, although polymer does not exist when the crystallization occurs.

Our 0.7PZN$-$0.3PT films have high dielectric constant and exhibit typical ferroelectric hysteresis loops. The dielectric constant and loss of the film on the conductive LNO-coated LAO substrate are 1570 and 0.06 at 1 kHz, respectively. The remnant polarization and coercive field are 12 $\mu C/cm^2$ and 100 kV/cm, respectively. The effective piezoelectric constant d_{33} is 50.6 pm/V at 1.5 kHz without taking into account the clamping effect of the substrate.

To the best of our knowledge, this is the first time that good ferroelectric and piezoelectric properties are obtained in perovskite phase $(1-x)$PZN$-x$PT thin films with (001) orientation and a composition close to MPB ($x \sim 0.1$). The understanding on the mechanism of PEG in promoting the formation of the perovskite phase while suppressing the pyrochlore phase developed in this study can apply to all the Pb-contained perovskite materials. This study thus provides a guideline about how to obtain the Pb-based perovskite phase in the ABO_3 systems which often show the preferential formation of pyrochlore phase.

Acknowledgment. The authors thank Dr. Pan Jisheng, Mr. Ong Zhun Yong, Mr. Lim Poh Chong, and Mr. He Xujiang for their assistance in carrying out the experiments and for helpful discussions.

CM052536V